Editors' Suggestion

High-Pressure Synthesis of Dirac Materials: Layered van der Waals Bonded BeN_4 Polymorph

Maxim Bykov,[1,2,*] Timofey Fedotenko,[3] Stella Chariton,[4] Dominique Laniel,[3] Konstantin Glazyrin,[5] Michael Hanfland,[6] Jesse S. Smith,[7] Vitali B. Prakapenka,[4] Mohammad F. Mahmood,[2] Alexander F. Goncharov,[1] Alena V. Ponomareva,[8] Ferenc Tasnádi,[9] Alexei I. Abrikosov,[10] Talha Bin Masood,[10] Ingrid Hotz,[10] Alexander N. Rudenko,[12,11,13] Mikhail I. Katsnelson,[12,13] Natalia Dubrovinskaia,[3,9] Leonid Dubrovinsky,[14,†] and Igor A. Abrikosov[9,‡]

[1]*The Earth and Planets Laboratory, Carnegie Institution for Science, Washington, D.C. 20015, USA*
[2]*College of Arts and Science, Howard University, Washington, D.C. 20059, USA*
[3]*Material Physics and Technology at Extreme Conditions, Laboratory of Crystallography, University of Bayreuth, 95440 Bayreuth, Germany*
[4]*Center for Advanced Radiation Sources, University of Chicago, Chicago, Illinois 60637, USA*
[5]*Photon Sciences, Deutsches Electronen Synchrotron (DESY), D-22607 Hamburg, Germany*
[6]*European Synchrotron Radiation Facility, 38043 Grenoble Cedex 9, France*
[7]*HPCAT, X-ray Science Division, Argonne National Laboratory, Argonne, Illinois 60439, USA*
[8]*Materials Modeling and Development Laboratory, National University of Science and Technology "MISIS," 119049 Moscow, Russia*
[9]*Department of Physics, Chemistry and Biology (IFM), Linköping University, SE-58183 Linköping, Sweden*
[10]*Department of Science and Technology (ITN), Linköping University, SE-60174 Norrköping, Sweden*
[11]*Key Laboratory of Artificial Micro- and Nano-Structures of Ministry of Education and School of Physics and Technology, Wuhan University, Wuhan 430072, China*
[12]*Radboud University, Institute for Molecules and Materials, 6525AJ Nijmegen, The Netherlands*
[13]*Department of Theoretical Physics and Applied Mathematics, Ural Federal University, 620002 Ekaterinburg, Russia*
[14]*Bayerisches Geoinstitut, University of Bayreuth, 95440 Bayreuth, Germany*

(Received 30 November 2020; revised 16 January 2021; accepted 24 March 2021; published 26 April 2021)

High-pressure chemistry is known to inspire the creation of unexpected new classes of compounds with exceptional properties. Here, we employ the laser-heated diamond anvil cell technique for synthesis of a Dirac material BeN_4. A triclinic phase of beryllium tetranitride tr-BeN_4 was synthesized from elements at ~85 GPa. Upon decompression to ambient conditions, it transforms into a compound with atomic-thick BeN_4 layers interconnected via weak van der Waals bonds and consisting of polyacetylene-like nitrogen chains with conjugated π systems and Be atoms in square-planar coordination. Theoretical calculations for a single BeN_4 layer show that its electronic lattice is described by a slightly distorted honeycomb structure reminiscent of the graphene lattice and the presence of Dirac points in the electronic band structure at the Fermi level. The BeN_4 layer, i.e., beryllonitrene, represents a qualitatively new class of 2D materials that can be built of a metal atom and polymeric nitrogen chains and host anisotropic Dirac fermions.

DOI: 10.1103/PhysRevLett.126.175501

The use of nonconventional methods of materials synthesis or established synthesis techniques in a nontrivial way may lead to breakthrough discoveries that revolutionize many research fields. One of the most striking examples is graphene. It was considered as an interesting two-dimensional (2D) model, though predominantly theoretical, before high quality graphitic films were derived by Novoselov *et al.* by mechanical exfoliation of small mesas of highly oriented pyrolytic graphite using adhesive tape [1]. Graphene is a material with gapless Dirac cones near the Fermi level with a linear energy-momentum dispersion near the Dirac points, and exhibiting ultrahigh carrier mobility. While the Dirac cones in graphene and many other 2D compounds are isotropic, their anisotropy could result in anisotropic carrier mobility, making it possible to realize direction-dependent quantum devices and motivating an intense search for materials systems hosting the anisotropic Dirac cones. Experimental evidence of anisotropic Dirac fermions has been reported in bulk stoichiometric $PtTe_2$ single crystal [2] and in 2D material borophene [3]. However, the Dirac point in these materials is far from the Fermi energy. A cone with its apex located near the Fermi level has been observed in $BaFe_2As_2$ [4], though the anisotropy was weak. There were theoretical predictions for the organic conductor α-$(BEDT\text{-}TTF)_2I_3$ at high pressure [5] and a B_2S honeycomb monolayer [6]. There are proposals to achieve desired anisotropy using mechanical stress, external periodic potentials,

heterostructures, or by a strong laser field [5–11]. However, experimental realization of a material hosting strongly anisotropic Dirac fermions at the Fermi energy is limited to a few examples [12,13] and calls for novel synthetic approaches.

The simplest design route of novel 2D materials is based on the substitution of elements in a known 2D material with its neighboring elements in the periodic table, for example the replacement of the carbon atom in graphene by boron and nitrogen leads to *h*-BN. Even more structural diversity and possible anisotropy may be achieved by considering the second-order neighbors, e.g., the hypothetical compound BeN_2 would have the same number of valence electrons as graphene but is intrinsically anisotropic in nature. The search of new 2D materials commonly starts with selecting of a known 3D precursor phase, most often thermodynamically stable or very long-lived metastable at ambient conditions, typically with a layered crystal structure with hexagonal motives. Such precursors are not currently available for the Be-N system, although, several compounds in the Be-N system were explored theoretically as potential 2D materials [14–16].

Nitrides possess the largest thermodynamic scale of metastability in terms of the energy differences between stable and metastable structures (~190 meV/atom), which may allow the kinetic stabilization of potentially useful compounds [17]. The synthesis of nitrogen-rich compounds is complicated by the great stability of the dinitrogen molecule N_2: the nitrides tend to decompose at relatively low temperatures, that may be below the temperatures that are required for the synthesis. One way to overcome this problem is to use the high-pressure conditions [18–22]. Furthermore, high pressure is a useful tool to affect the bonding types, coordination environments, and physical properties of compounds, which may lead to completely unexpected results. For example, beryllium, known to be tetrahedrally coordinated in inorganic compounds, was recently reported to incrementally change its coordination number from four to six in the crystal structure of $CaBe_2P_2O_8$ under compression [23]. Thus, potentially, the high-pressure synthesis of a beryllium nitride with octahedrally coordinated Be may provide room for unexpected structural changes on decompression. In this Letter we report the exploration of this pathway through the investigation of beryllium polynitrides.

High-pressure high-temperature chemical reactions in the Be-N system were studied in laser-heated diamond anvil cells (LHDACs) using synchrotron powder and single-crystal x-ray diffraction (Methods, Table S1 [23]). The experiments led to a synthesis of several Be polynitrides (Fig. 1 and Supplemental Material, Figs. S1, S2, Table S2 [23]). In particular, at 84 GPa and ~2000 K, laser heating of Be and N_2 resulted in the synthesis of a compound with the chemical composition BeN_4 and a triclinic structure, further referred to as tr-BeN_4. The full crystallographic information for this compound is given in Supplemental Material, Table S3 [24]. The Be atom is coordinated by six nitrogen atoms forming an elongated

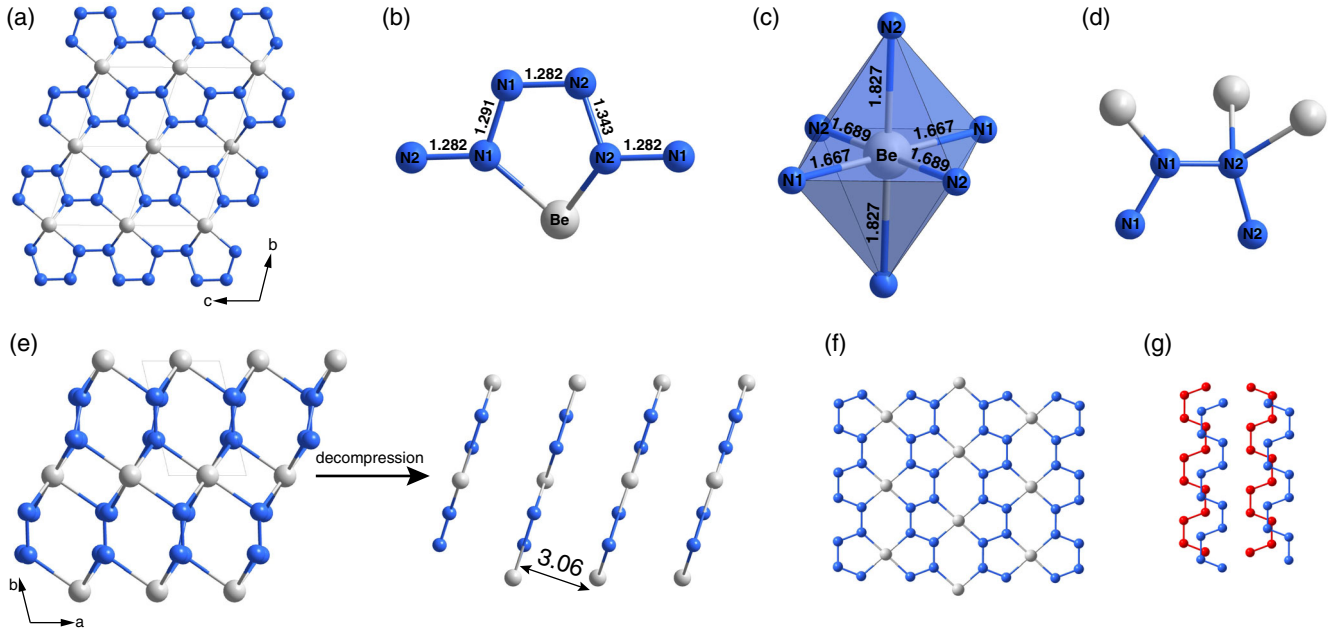

FIG. 1. Crystal structure of tr-BeN_4 at 84 GPa. (a) The view along the [100] direction; (b) coordination of a Be atom by one of the polymeric nitrogen chains. (c) BeN_6 octahedron with Be-N distances given in Å. (d) Coordination geometry of the nitrogen chain. (e) Scheme showing the transformation of tr-BeN_4 upon decompression. (f) Single layer of BeN_4 at ambient pressure. (g) Stacking sequence of polymeric nitrogen chains belonging to neighboring layers of tr-BeN_4 at ambient pressure; viewing direction is perpendicular to the layer. Beryllium and nitrogen atoms are represented as gray and blue spheres, respectively.

octahedron. The covalently bonded nitrogen atoms form infinite zigzag chains running along the [001] direction [Fig. 1(a)]. If viewed along the [001] direction [Fig. 1(e)], the structure can be understood as consisting of slightly corrugated BeN_4 layers, interconnected with each other by long Be-N bonds (∼1.83 Å). The tr-BeN_4 is isostructural with the FeN_4 compound, which was previously synthesized at ∼106 GPa from Fe and N_2 [61,62]. The metal-nitrogen bonds in BeN_4 have a slightly more ionic character than in FeN_4, which leads to a more uniform electron distribution within the polymeric chains (Fig. S3 [24]).

Theoretical calculations of the structural properties of tr-BeN_4 in a framework of density functional theory showed an excellent agreement between the theory and experiment for the lattice parameters, both at the synthesis pressure and on decompression (Fig. S4 [24]). Moreover, the structure is dynamically stable as indicated by the absence of the imaginary frequencies in the phonon dispersion calculations (Fig. S5 [24]). According to our calculated convex-hull diagram (Fig. S6 [24]) tr-BeN_4 remains thermodynamically stable down to at least 40 GPa and enters the metastability region upon further decompression.

On decompression the tr-BeN_4 produced excellent single-crystal diffraction patterns down to ∼60 GPa, but at lower pressures the crystal quality started to deteriorate. Since the theoretical model perfectly matches the experimental structure at high pressures and the evolution of the strongest and well-separated (010) reflection well agrees with that suggested theoretically (Fig. S4d [24]), the evolution of the structure below 60 GPa was tracked by powder XRD and compared with the results of calculations. The weakening of the diffraction signal and the significant overlapping of the strongest reflections of tr-BeN_4 with those of ε-N_2 upon pressure decrease prevented us from unambiguous refinement of all six unit cell parameters at 20 and 34 GPa. However, the refinement was successfully made at ambient pressure (Figs. S4, S7 [24]) after the DAC was fully decompressed and nitrogen released. The decompressed sample of tr-BeN_4 is a highly textured powder and it contains α-Be_3N_2, which was not observed at higher pressures. Therefore, we conclude that at ambient conditions tr-BeN_4 slowly decomposes into α-Be_3N_2 but could potentially be completely kinetically stabilized at slightly lower temperature or by keeping the sample in a nitrogen atmosphere. No evidence of amorphous products (e.g., liquid nitrogen) in the diffraction pattern show that nitrogen was completely released from the DAC and the sample was already in contact with atmosphere.

The structural evolution of tr-BeN_4 on decompression involves breaking of two longer Be-N bonds in the BeN_6 octahedra which leads to a change of the coordination of the Be atom from octahedral to square planar. Consequently, all nitrogen atoms become sp^2 hybridized and form infinite planar polyacetylenelike chains (Fig. 2 and Supplemental Material, Movie S1 [24]). The process of rearrangement becomes apparent below 50 GPa, as it can be judged from the interplanar distance (Fig. S4 [24]). The evolution of the structure to the layered motif, which is dynamically stable at ambient pressure (Fig. S5b [24]), is accompanied by a significant depletion of the electron density between the layers (Fig. 2 and Movie S1 [24]). The topological data analysis (see Supplemental Material, Methods [24]) confirms that the charge density value corresponding to the layers' separation decreases with decreasing pressure. Thus, the BeN_4 layers are more weakly connected at ambient pressure than at high pressure, indicating the formation of a van der Waals–bonded solid, as confirmed by our theoretical analysis of the interlayer bonding in tr-BeN_4 and the exfoliation energy at ambient pressure (see Methods [24]).

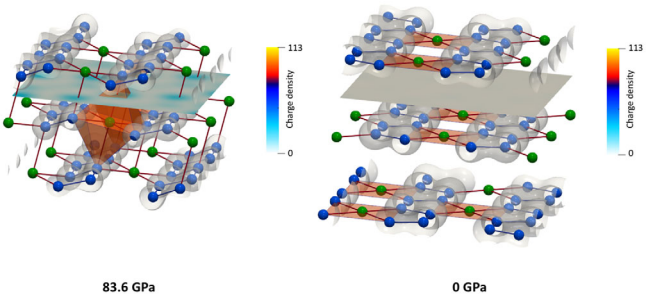

FIG. 2. Evolution of the crystal structure and the charge density of tr-BeN_4 upon decompression from the synthesis pressure to ambient. At the synthesis pressure, Be and N atoms form corrugated nets and the Be atoms (green) are octahedrally coordinated by six N atoms (blue) (left figure). Upon decompression, below about 50 GPa, the structure relaxes in such a way that the corrugated nets of Be and N atoms flatten, their increasing mutual separation reduces the coordination number of Be atoms to 4, thus turning the structure motif to layered (right figure). The gray planes between the layers indicate the position of the charge density slice and visualize the depletion of the charge density between two layers of tr-BeN_4 at zero pressure relative to that at synthesis pressure. Topological data analysis of the charge density (see Supplemental Material, Methods, Figs. S10–S11 [24]) confirms a stronger interaction within layers and weaker interaction between layers as the pressure is decreased. Experimental lattice parameters for tr-BeN_4 at 1 bar: $a = 3.275(2)$, $b = 4.212(2)$, $c = 3.704(2)$ Å, $\alpha = 103.43(3)$, $\beta = 105.61(4)$, $\gamma = 111.86(4)°$, $V = 42.4$ Å^3. Optimized atomic positions: Be (0.5 0 0), N1 (0.1592 0.66170 0.5144), N2 (0.15840 0.6630 0.14780).

Electronic structure calculations (Fig. S8 [24]) show that both the high pressure and the ambient pressure modifications of tr-BeN_4 are metallic. The calculated electron density maps and electron localization functions at a pressure of $P \sim 85$ GPa (Fig. S9 [24]) indicate a nonuniform distribution of electron density between the nitrogen atoms of the chains, in agreement with the crystal-chemical analysis (Fig. S3 [24]). During decompression, the electron density and interatomic distances become

almost the same between all the atoms of the nitrogen chains, and the chains become planar (Fig. S9 [24]). Similar planar polyacetylenelike nitrogen chains with conjugated π systems were recently observed in a series of metal-inorganic frameworks Hf_4N_{22}, WN_{10}, ReN_{10}, Os_5N_{34} [63,64], and MgN_4 [65].

The high-pressure synthesis is a well established path for the discovery of novel materials. A normal high-pressure synthesis route includes pressurizing and heating in the stability field of a new compound followed by its recovery to ambient pressure, hoping to preserve the material's interesting properties [66,67]. In this respect tr-BeN_4 is an exciting exception, as its layered ambient-pressure modification obtained upon decompression appears to possess even more intriguing properties than one could expect from the high-pressure one. Its bulk electronic structure is modified in a remarkable fashion upon the decompression: one can clearly see the development of a pronounced pseudogap at the Fermi energy in tr-BeN_4 at low pressure. A closer examination of the bulk band structure and the Fermi surface (Fig. S8, Movie S2 [24]) allows us to conclude that there are two nodal points in the Brillouin zone (BZ) of tr-BeN_4 located at the Fermi energy. Given that both time-reversal and inversion symmetry are preserved, the two points are fourfold degenerate, indicating that they correspond to the Dirac points. The breaking of the inversion symmetry would split each of these points into Weyl points [68]. Though the electronic DOS in bulk tr-BeN_4 is finite, it originates from the well-defined Fermi surface pockets (electron and hole). Going from 3D to 2D, those pockets vanish, leaving only the Dirac points in the whole BZ. This makes the layered modification of tr-BeN_4 obtained upon decompression a precursor for a new anisotropic 2D Dirac material, the beryllonitrene. Our estimation of the exfoliation energy of the single monolayer for tr-BeN_4 (see Methods [24]) indicates that it is indeed possible.

The main interest in fundamental studies and potential applications of 2D materials is related to their peculiar electronic properties. Therefore, we now turn to the electronic structure of the beryllonitrene. The optimized crystal structure of single-layer BeN_4 is shown in Fig. 3(a). It belongs to the oblique crystal system (the two-dimensional space group $p2$). The corresponding electronic band structure and density of states (DOS) are shown in Fig. 3(b). One can see that unlike bulk tr-BeN_4, the beryllonitrene is a Dirac semimetal with linear dispersion in the vicinity of the Fermi energy and two Dirac points coinciding with the Fermi energy, similar to graphene. Around the Fermi energy, electron, and hole states are essentially symmetric over an energy range of roughly 2 eV. It is this property rather than the conical point itself which opens a way to deep relations to high-energy physics within its symmetry between particles and antiparticles [69]. Unlike graphene, the Dirac points are not located at the corners of the BZ, but rather along the Γ-A direction (Σ point) as shown in the inset of Fig. 3(b). This can be attributed to a lower symmetry of the BeN_4 lattice compared to graphene. Indeed, one can see that the dispersion is different along the Σ-Γ and Σ-A directions, demonstrating a pronounced anisotropy of the band structure even in the long-wavelength limit.

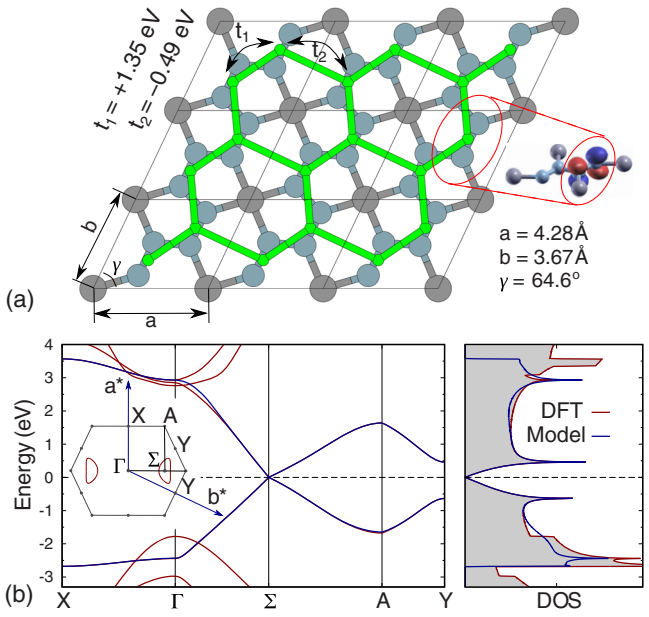

FIG. 3. Electronic structure of the beryllonitrene (a) Effective electronic lattice (green) superimposed onto the real-space crystal structure of single-layer BeN_4 (a) Green balls centered on the N-N bond correspond to the wave functions shown on the right side. Fourfold-coordinated gray balls depict Be atoms, dirty-blue threefold coordinated balls correspond to N atoms. Arrows denote two main interaction parameters defined in terms of a tight-binding Hamiltonian. (b) Electronic band structure and the density of states calculated using DFT (red) and the *electronic* lattice model (blue) shown in (a). The inset shows the Brillouin zone with the high-symmetry points, as well as the Fermi surface corresponding to the Fermi energy of −0.5 eV.

From the calculated band structure one can immediately estimate the carrier velocities in single-layer BeN_4 as $v(\boldsymbol{k}) = (1/\hbar)[\partial E(\mathbf{k})/\partial \mathbf{k}]$. Along the Σ-Γ direction, we find the Fermi velocity to be $v_y = 0.8 \times 10^6$ m/s, which is 1.3 times smaller than the Fermi velocity in graphene [70,71]. Along the Σ-A direction, the Fermi velocity is essentially smaller ($v_x = 0.3 \times 10^6$ m/s). At small charge doping the Fermi surface is elliptical with the dispersion given by $E(\boldsymbol{k}) = \hbar(v_x^2 k_x^2 + v_y^2 k_y^2)^{1/2}$. The anisotropy of the Fermi velocities is also reflected in the Fermi surface shown in the inset of Fig. 3(b). At sufficiently high doping, the Fermi surface is not elliptical, but is represented by two oppositely oriented semicircles. It is worth noting that in this case the Fermi surface is perfectly nested by the wave vectors connecting two parallel parts of the two Fermi surface pockets. Therefore, the intervalley scattering in doped single-layer BeN_4 is expected to be strongly anisotropic.

To gain more insights into the physics of beryllonitrene, we construct a minimal lattice electronic model which describes its band structure (see Supplemental Material, Methods [24]). The corresponding "effective lattice" (electronic structure model) is shown in Fig. 3(a) superimposed onto the real-space crystal structure. It is described by a slightly distorted honeycomb net reminiscent to that of graphene. Each node of the honeycomb net is located at the center of the N-N bond. The model allows us to assess the relevance of screening effects in single-layer BeN_4. Calculations show (see Methods [24]) that at small wave vectors the static dielectric function $\varepsilon \approx 8$ is notably larger compared to graphene (3.5), suggesting that the screening effects are more pronounced in beryllonitrene. Another essential difference with graphene is the existence of van Hove singularities close enough to the Fermi energy (the separation is about 0.5 eV, contrary to approximately 2 eV in graphene). One can assume that this van Hove singularity is available by a reasonable doping; the Fermi energy shift by 0.5 eV is relatively easily reachable in graphene by chemical doping [72]. Recently, an even much higher shift, about 2 eV, was reached in graphene by Gd intercalation [73]. In 2D systems with a Fermi energy close enough to the van Hove singularity one can expect the formation of flat bands and strong Fermi surface nesting. Because of many-body effects, this may result in all kinds of correlation-induced instabilities (see Ref. [74] and references therein), including, e.g., the emergence of superconducting or magnetic phases [75] as well as charge- or spin-density waves [76].

To conclude, applying high-pressure synthesis followed by decompression to ambient conditions, we have synthesized new layered material BeN_4. As shown by van der Waals bonds between its layers and the presence of anisotropic Dirac cones in its electronic structure, 2D BeN_4, beryllonitrene, has unique properties. Indeed, the high degree of electron-hole symmetry makes the 2D BeN_4 system similar, in some respect, to the world of high-energy particles with its symmetry between particles and antiparticles. However, contrary to the "true" Universe, which is isotropic, the massless Dirac fermions in the beryllonitrene are essentially anisotropic (see Methods [24]). This opens a door into the whole new world and the question arises on modification of "conventional" quantum relativistic effects such as Zitterbewegung, chiral tunneling, relativistic collapse at supercritical charges etc. [69] for the *anisotropic* massless fermions. We demonstrate the experimental realization of tr-BeN_4 in a diamond anvil cell and believe that further experiments aiming to control the quantity of the material or the crystallite size will allow the experimental realization of 2D beryllonitrene. Because of the relatively low nitrogen content in BeN_4 it potentially could be synthesized from beryllium azide $Be(N_3)_2$, which would not require a direct reaction between beryllium and nitrogen.

Parts of this research were carried out at the Extreme Conditions Beamline (P02.2) at DESY, a member of Helmholtz Association (HGF). Portions of this work were performed on beamline ID15 at the European Synchrotron Radiation Facility (ESRF), Grenoble, France. Portions of this work were performed at GeoSoilEnviroCARS (The University of Chicago, Sector 13) and at HPCAT (sector 16) of the Advanced Photon Source (APS), Argonne National Laboratory. Research was sponsored by the Army Research Office and was accomplished under the Cooperative Agreement No. W911NF-19-2-0172. N. D. and L. D. thank the Deutsche Forschungsgemeinschaft (DFG Projects No. DU 954-11/1, No. DU 393-9/2, and No. DU 393-13/1) and the Federal Ministry of Education and Research, Germany (BMBF, Grant No. No. 05K19WC1) for financial support. D. L. thanks the Alexander von Humboldt Foundation for financial support. Theoretical analysis of chemical bonding was supported by the Russian Science Foundation (Project No. 18-12-00492). Calculations of the phonon dispersion relations were supported by the Ministry of Science and Higher Education of the Russian Federation in the framework of Increase Competitiveness Program of NUST MISIS (No. K2-2020-026) implemented by governmental decree No. 211. Support from the Knut and Alice Wallenberg Foundation (Wallenberg Scholar Grant No. KAW-2018.0194), the Swedish Government Strategic Research Areas in Materials Science on Functional Materials at Linköping University (Faculty Grant SFO-Mat-LiU No. 2009 00971) and SeRC, the Swedish Research Council (VR) Grant No. 2019-05600 and Vinnova VINN Excellence Center Functional Nanoscale Materials (FunMat-2) Grant No. 2016–05156 is gratefully acknowledged. The computations were enabled by resources provided by the Swedish National Infrastructure for Computing (SNIC) partially funded by the Swedish Research Council through Grant Agreement No. 2016-07213. The work of M. I. K. was supported by the JTC-FLAGERA Project GRANSPORT. GeoSoilEnviroCARS is supported by the National Science Foundation–Earth Sciences (EAR–1634415) and Department of Energy-Geosciences (DE-FG02-94ER14466). HPCAT operations are supported by DOE-NNSA's Office of Experimental Sciences. Advanced Photon Source is U.S. Department of Energy (DOE) Office of Science User Facility operated for the DOE Office of Science by Argonne National Laboratory under Contract No. DE-AC02-06CH11357.

*Corresponding author.
maks.byk@gmail.com
†Corresponding author.
leonid.dubrovinsky@uni-bayreuth.de

‡Corresponding author.
igor.abrikosov@liu.se

[1] K. S. Novoselov, A. K. Geim, S. V. Morozov, Y. Jiang, S. V. Dubonos, I. V. Grigorieva, and A. A. Firsov, Science **306**, 666 (2004).
[2] M. Yan, H. Huang, K. Zhang, E. Wang, W. Yao, K. Deng, G. Wan, H. Zhang, M. Arita, H. Yang, Z. Sun, H. Yao, Y. Wu, S. Fan, W. Duan, and S. Zhou, Nat. Commun. **8**, 257 (2017).
[3] B. Feng, O. Sugino, R.-Y. Liu, J. Zhang, R. Yukawa, M. Kawamura, T. Iimori, H. Kim, Y. Hasegawa, H. Li, L. Chen, K. Wu, H. Kumigashira, F. Komori, T.-C. Chiang, S. Meng, and I. Matsuda, Phys. Rev. Lett. **118**, 096401 (2017).
[4] P. Richard, K. Nakayama, T. Sato, M. Neupane, Y.-M. Xu, J. H. Bowen, G. F. Chen, J. L. Luo, N. L. Wang, X. Dai, Z. Fang, H. Ding, and T. Takahashi, Phys. Rev. Lett. **104**, 137001 (2010).
[5] Y. Suzumura, J. Phys. Soc. Jpn. **85**, 053708 (2016).
[6] Y. Zhao, X. Li, J. Liu, C. Zhang, and Q. Wang, J. Phys. Chem. Lett. **9**, 1815 (2018).
[7] S.-M. Choi, S.-H. Jhi, and Y.-W. Son, Phys. Rev. B **81**, 081407(R) (2010).
[8] C.-H. Park, L. Yang, Y.-W. Son, M. L. Cohen, and S. G. Louie, Nat. Phys. **4**, 213 (2008).
[9] S. Katayama, A. Kobayashi, and Y. Suzumura, J. Phys. Soc. Jpn. **75**, 054705 (2006).
[10] M. Ezawa, Phys. Rev. Lett. **110**, 026603 (2013).
[11] C. Dutreix, E. A. Stepanov, and M. I. Katsnelson, Phys. Rev. B **93**, 241404(R) (2016).
[12] J. Kim, S. S. Baik, S. H. Ryu, Y. Sohn, S. Park, B.-G. Park, J. Denlinger, Y. Yi, H. J. Choi, and K. S. Kim, Science **349**, 723 (2015).
[13] X. Yuan, C. Zhang, Y. Liu, A. Narayan, C. Song, S. Shen, X. Sui, J. Xu, H. Yu, Z. An, J. Zhao, S. Sanvito, H. Yan, and F. Xiu, NPG Asia Mater. **8**, e325 (2016).
[14] C. Chen, B. Huang, and J. Wu, AIP Adv. **8**, 105105 (2018).
[15] C. Zhang and Q. Sun, J. Phys. Chem. Lett. **7**, 2664 (2016).
[16] Y. Ding, Y. Ji, H. Dong, N. Rujisamphan, and Y. Li, Nanotechnology **30**, 465202 (2019).
[17] W. Sun, S. T. Dacek, S. P. Ong, G. Hautier, A. Jain, W. D. Richards, A. C. Gamst, K. A. Persson, and G. Ceder, Sci. Adv. **2**, e1600225 (2016).
[18] B. A. Steele, E. Stavrou, J. C. Crowhurst, J. M. Zaug, V. B. Prakapenka, and I. I. Oleynik, Chem. Mater. **29**, 735 (2017).
[19] M. Bykov, K. R. Tasca, I. G. Batyrev, D. Smith, K. Glazyrin, S. Chariton, M. Mahmood, and A. F. Goncharov, Inorg. Chem. **59**, 14819 (2020).
[20] K. Niwa, T. Terabe, K. Suzuki, Y. Shirako, and M. Hasegawa, J. Appl. Phys. **119**, 065901 (2016).
[21] M. Bykov, K. V. Yusenko, E. Bykova, A. Pakhomova, W. Kraus, N. Dubrovinskaia, and L. Dubrovinsky, Eur. J. Inorg. Chem. **2019**, 3667 (2019).
[22] M. Bykov, E. Bykova, A. V. Ponomareva, I. A. Abrikosov, S. Chariton, V. B. Prakapenka, M. F. Mahmood, L. Dubrovinsky, and A. F. Goncharov, Angew. Chem Int. Ed. (2021), https://doi.org/10.1002/anie.202100283.
[23] A. Pakhomova, G. Aprilis, M. Bykov, L. Gorelova, S. S. Krivovichev, M. P. Belov, I. A. Abrikosov, and L. Dubrovinsky, Nat. Commun. **10**, 2800 (2019).
[24] See Supplemental Material at http://link.aps.org/supplemental/10.1103/PhysRevLett.126.175501 for methods, crystal structure details of tr-BeN_4 and m-BeN_4, phonon dispersions, convex-hull diagram for the Be-N system, electronic band structures, density of states, charge density maps, electron localization functions, and topological charge density analysis of tr-BeN_4, which includes Refs. [25–60].
[25] C. Prescher and V. B. Prakapenka, High Press. Res. **35**, 223 (2015).
[26] V. Petricek, M. Dusek, and L. Palatinus, Z. Krist. **229**, 345 (2014).
[27] G. M. Sheldrick, Acta Crystallogr. Sect. A **71**, 3 (2015).
[28] G. M. Sheldrick, Acta Crystallogr. Sect. A **64**, 112 (2008).
[29] O. V. Dolomanov, L. J. Bourhis, R. J. Gildea, J. A. K. Howard, and H. Puschmann, J. Appl. Crystallogr. **42**, 339 (2009).
[30] J. Gonzalez-Platas, M. Alvaro, F. Nestola, and R. Angel, J. Appl. Crystallogr. **49**, 1377 (2016).
[31] P. E. Blöchl, Phys. Rev. B **50**, 17953 (1994).
[32] G. Kresse and J. Furthmüller, Comput. Mater. Sci. **6**, 15 (1996).
[33] G. Kresse and J. Furthmüller, Phys. Rev. B **54**, 11169 (1996).
[34] G. Kresse and D. Joubert, Phys. Rev. B **59**, 1758 (1999).
[35] J. P. Perdew, K. Burke, and M. Ernzerhof, Phys. Rev. Lett. **77**, 3865 (1996).
[36] J. Klimeš, D. R. Bowler, and A. Michaelides, Phys. Rev. B **83**, 195131 (2011).
[37] J. Klimeš, D. R. Bowler, and A. Michaelides, J. Phys. Condens. Matter **22**, 022201 (2010).
[38] A. Togo and I. Tanaka, Scr. Mater. **108**, 1 (2015).
[39] H. Carr, J. Snoeyink, and U. Axen, Comput. Geom. **24**, 75 (2003).
[40] C. Heine, H. Leitte, M. Hlawitschka, F. Iuricich, L. De Floriani, G. Scheuermann, H. Hagen, and C. Garth, Computer Graphics Forum **35**, 643 (2016).
[41] R. F. W. Bader, *Atoms in Molecules: A Quantum Theory* (Clarendon Press, Oxford, 1994).
[42] W. Wang, S. Dai, X. Li, J. Yang, D. J. Srolovitz, and Q. Zheng, Nat. Commun. **6**, 7853 (2015).
[43] J. Wang, D. C. Sorescu, S. Jeon, A. Belianinov, S. V. Kalinin, A. P. Baddorf, and P. Maksymovych, Nat. Commun. **7**, 13263 (2016).
[44] Y. Han, K. C. Lai, A. Lii-Rosales, M. C. Tringides, J. W. Evans, and P. A. Thiel, Surf. Sci. **685**, 48 (2019).
[45] N. Marzari, A. A. Mostofi, J. R. Yates, I. Souza, and D. Vanderbilt, Rev. Mod. Phys. **84**, 1419 (2012).
[46] A. A. Mostofi, J. R. Yates, Y.-S. Lee, I. Souza, D. Vanderbilt, and N. Marzari, Comput. Phys. Commun. **178**, 685 (2008).
[47] N. Y. Astrakhantsev, V. V. Braguta, M. I. Katsnelson, A. A. Nikolaev, and M. V. Ulybyshev, Phys. Rev. B **97**, 035102 (2018).
[48] V. K. Dugaev and M. I. Katsnelson, Phys. Rev. B **86**, 115405 (2012).
[49] F. Aryasetiawan, M. Imada, A. Georges, G. Kotliar, S. Biermann, and A. I. Lichtenstein, Phys. Rev. B **70**, 195104 (2004).
[50] T. O. Wehling, E. Şaşıoğlu, C. Friedrich, A. I. Lichtenstein, M. I. Katsnelson, and S. Blügel, Phys. Rev. Lett. **106**, 236805 (2011).
[51] M. V. Ulybyshev, P. V. Buividovich, M. I. Katsnelson, and M. I. Polikarpov, Phys. Rev. Lett. **111**, 056801 (2013).

[52] J. González, F. Guinea, and M. A. H. Vozmediano, Nucl. Phys. **B424**, 595 (1994).
[53] H. E. Maynard-Casely, J. R. Hester, and H. E. A. Brand, IUCrJ **7**, 844 (2020).
[54] H. Olijnyk, J. Chem. Phys. **93**, 8968 (1990).
[55] M. I. Eremets, A. G. Gavriliuk, I. A. Trojan, D. A. Dzivenko, and R. Boehler, Nat. Mater. **3**, 558 (2004).
[56] S. Zhang, Z. Zhao, L. Liu, and G. Yang, J. Power Sources **365**, 155 (2017).
[57] J. Lin, Z. Zhu, Q. Jiang, S. Guo, J. Li, H. Zhu, and X. Wang, AIP Adv. **9**, 055116 (2019).
[58] S. R. Römer, T. Dörfler, P. Kroll, and W. Schnick, Phys. Status Solidi **246**, 1604 (2009).
[59] Y. Zhang, H. Wang, Y. Wang, L. Zhang, and Y. Ma, Phys. Rev. X **7**, 011017 (2017).
[60] S. Anzellini, A. Dewaele, F. Occelli, P. Loubeyre, and M. Mezouar, J. Appl. Phys. **115**, 043511 (2014).
[61] M. Bykov, E. Bykova, G. Aprilis, K. Glazyrin, E. Koemets, I. Chuvashova, I. Kupenko, C. McCammon, M. Mezouar, V. Prakapenka, H.-P. Liermann, F. Tasnádi, A. V. Ponomareva, I. A. Abrikosov, N. Dubrovinskaia, and L. Dubrovinsky, Nat. Commun. **9**, 2756 (2018).
[62] M. Bykov, S. Khandarkhaeva, T. Fedotenko, P. Sedmak, N. Dubrovinskaia, and L. Dubrovinsky, Acta Crystallogr. Sect. E **74**, 1392 (2018).
[63] M. Bykov, S. Chariton, E. Bykova, S. Khandarkhaeva, T. Fedotenko, A. V. Ponomareva, J. Tidholm, F. Tasnádi, I. A. Abrikosov, P. Sedmak, V. Prakapenka, M. Hanfland, H.-P. Liermann, M. Mahmood, A. F. Goncharov, N. Dubrovinskaia, and L. Dubrovinsky, Angew. Chem., Int. Ed. Engl. **59**, 10321 (2020).
[64] M. Bykov, E. Bykova, E. Koemets, T. Fedotenko, G. Aprilis, K. Glazyrin, H.-P. P. Liermann, A. V. Ponomareva, J. Tidholm, F. Tasnádi, I. A. Abrikosov, N. Dubrovinskaia, and L. Dubrovinsky, Angew. Chem., Int. Ed. Engl. **57**, 9048 (2018).
[65] D. Laniel, B. Winkler, E. Koemets, T. Fedotenko, M. Bykov, E. Bykova, L. Dubrovinsky, and N. Dubrovinskaia, Nat. Commun. **10**, 4515 (2019).
[66] M. Bykov, S. Chariton, H. Fei, T. Fedotenko, G. Aprilis, A. V. Ponomareva, F. Tasnádi, I. A. Abrikosov, B. Merle, P. Feldner, S. Vogel, W. Schnick, V. B. Prakapenka, E. Greenberg, M. Hanfland, A. Pakhomova, H.-P. Liermann, T. Katsura, N. Dubrovinskaia, and L. Dubrovinsky, Nat. Commun. **10**, 2994 (2019).
[67] P. F. McMillan, Nat. Mater. **1**, 19 (2002).
[68] S. M. Young, S. Zaheer, J. C. Y. Teo, C. L. Kane, E. J. Mele, and A. M. Rappe, Phys. Rev. Lett. **108**, 140405 (2012).
[69] M. I. Katsnelson, *The Physics of Graphene*, 2nd ed. (Cambridge University Press, Cambridge, England, 2020).
[70] K. S. Novoselov, A. K. Geim, S. V. Morozov, D. Jiang, M. I. Katsnelson, I. V. Grigorieva, S. V. Dubonos, and A. A. Firsov, Nature (London) **438**, 197 (2005).
[71] Y. Zhang, Y.-W. Tan, H. L. Stormer, and P. Kim, Nature (London) **438**, 201 (2005).
[72] R. R. Nair, I.-L. Tsai, M. Sepioni, O. Lehtinen, J. Keinonen, A. V. Krasheninnikov, A. H. Castro Neto, M. I. Katsnelson, A. K. Geim, and I. V. Grigorieva, Nat. Commun. **4**, 2010 (2013).
[73] S. Link, S. Forti, A. Stöhr, K. Küster, M. Rösner, D. Hirschmeier, C. Chen, J. Avila, M. C. Asensio, A. A. Zakharov, T. O. Wehling, A. I. Lichtenstein, M. I. Katsnelson, and U. Starke, Phys. Rev. B **100**, 121407(R) (2019).
[74] D. Yudin, D. Hirschmeier, H. Hafermann, O. Eriksson, A. I. Lichtenstein, and M. I. Katsnelson, Phys. Rev. Lett. **112**, 070403 (2014).
[75] V. Y. Irkhin, A. A. Katanin, and M. I. Katsnelson, Phys. Rev. B **64**, 165107 (2001).
[76] P. Monceau, Adv. Phys. **61**, 325 (2012).